Cellular Signalling 81 (2021) 109928

Contents lists available at ScienceDirect

Cellular Signalling

journal homepage: www.elsevier.com/locate/cellsig

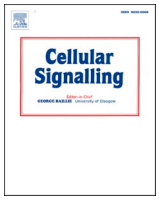

Myriocin modulates the altered lipid metabolism and storage in cystic fibrosis

Paola Signorelli [a,b], Francesca Pivari [a], Matteo Barcella [c], Ivan Merelli [d], Aida Zulueta [a], Michele Dei Cas [e], Lorenzo Rosso [f], Riccardo Ghidoni [a,b], Anna Caretti [a], Rita Paroni [e], Alessandra Mingione [a,b,*]

[a] Biochemistry and Molecular Biology Laboratory, Department of Health Science, University of Milan, Milan, Italy
[b] "Aldo Ravelli" Center for Neurotechnology and Experimental Brain Therapeutics, University of Milan, Milan, Italy
[c] Department of Health Sciences, University of Milan, Milan, Italy
[d] Institute for Biomedical Technologies, National Research Council of Italy, Milan, Italy
[e] Laboratory of Clinical Biochemistry and Mass Spectrometry, Department of Health Sciences, University of Milan, Milan, Italy
[f] Thoracic surgery and transplantation Unit, Fondazione IRCCS Ca Granda Ospedale Maggiore Policlinico, Health Sciences Department, University of Milan, Milan, Italy

ARTICLE INFO

Keywords:
Cystic fibrosis
Sphingolipids
Myriocin
Lipid droplet
Lipid metabolism

ABSTRACT

Cystic fibrosis (CF) is a hereditary disease mostly related to ΔF508 CFTR mutation causing a proteinopathy that is characterized by multiple organ dysfunction, primarily lungs chronic inflammation, and infection. Defective autophagy and accumulation of the inflammatory lipid ceramide have been proposed as therapeutic targets. Accumulation of lipids and cholesterol was reported in the airways of CF patients, together with altered triglycerides and cholesterol levels in plasma, thus suggesting a disease-related dyslipidemia. Myriocin, an inhibitor of sphingolipids synthesis, significantly reduces inflammation and activates TFEB-induced response to stress, enhancing fatty acids oxidation and promoting autophagy. Myriocin ameliorates the response against microbial infection in CF models and patients' monocytes. Here we show that CF broncho-epithelial cells exhibit an altered distribution of intracellular lipids. We demonstrated that lipid accumulation is supported by an enhanced synthesis of fatty acids containing molecules and that Myriocin is able to reduce such accumulation. Moreover, Myriocin modulated the transcriptional profile of CF cells in order to restore autophagy, activate an antioxidative response, stimulate lipid metabolism and reduce lipid peroxidation. Moreover, lipid storage may be altered in CF cells, since we observed a reduced expression of lipid droplets related proteins named perilipin 3 and 5 and seipin. To note, Myriocin up-regulates the expression of genes that are involved in lipid droplets biosynthesis and maturation. We suggest that targeting sphingolipids de novo synthesis may counteract lipids accumulation by modulating CF altered transcriptional profile, thus restoring autophagy and lipid metabolism homeostasis.

Abbreviations: CF, Cystic Fibrosis; CFTR, Cystic Fibrosis Transmembrane Regulator; LDL, Low Density Lipoprotein; Myr, Myriocin; FA, Fatty Acids; LDs, Lipid Droplets; TAG, Triacylglycerol; ER, Endoplasmic Reticulum; OA, Oleic Acid; BSA, Bovine Serum Albumin; MDA, Malondialdehyde; GTF, Gene transfer file; GSEA, Gene Set Enrichment Analysis; DEG, Differentially Expressed Genes; GO, Gene Ontology; KEGG, Kyoto Encyclopedia of Genes and Genomes; MSigDB, Molecular Signatures Database; CPT1A, Carnitine Palmitoyl Transferase 1a; SREBF1, Sterol Regulatory Element Binding transcription Factor 1; PLINs, Perilipins; TFEB, Transcription Factor EB; PPARs, Peroxisome Proliferator Activated Receptors; NPC, Niemann-Pick C proteins; SNX14, Sorting Nexin 14; FITM2, Fat storage Inducing Transmembrane Protein 2; BSCL2, Seipin; NRF2, Nuclear Factor Erythroid 2; TBK1, TANK Binding Kinase 1; TP53INP, Tumor Protein P53 Inducible Nuclear Protein 1; TMEM59, Transmembrane protein 59; IL, Interleukin; CROT, Carnitine O-octanoyltransferase; ACAD, Acyl-CoA Dehydrogenase; ABHD, Abhydrolase Domain Containing Proteins; GPAT 3/4, Glycerol-3-phosphate acyltransferase ¾; LIP A, Lipase A; FASN, Fatty acid synthase; NCO, Nuclear Receptor Coactivator; MED, Mediator complex.

* Corresponding author at: Via di Rudinì 8, 20142 Milan, Italy.
E-mail address: alessandra.mingione@unimi.it (A. Mingione).

https://doi.org/10.1016/j.cellsig.2021.109928
Received 29 October 2020; Received in revised form 13 January 2021; Accepted 13 January 2021
Available online 19 January 2021

1. Introduction

Cystic fibrosis (CF) is characterized by multiple organs dysfunction, primarily lungs and pancreas, due to the mutation of the chloride/carbonate channel CFTR [1]. The 508-phenylalanine deletion is the prevalent mutation, encoded in 70% of mutant alleles in Caucasian patients, causing a proteinopathy, which is responsible for inducing oxidative stress and reduced autophagy. CF patients are characterized by chronic inflammation and the inability to clear airways infections [2] and pancreatic insufficiency. Along with the improvement of therapeutic strategies and the increase of life expectancy, the rate of comorbidities affecting CF patients is augmenting, including the less studied dyslipidemia. High triglycerides, low LDL and cholesterol levels have been identified in the plasma of CF patients [3–5], as well as peripheral tissue fat accumulation [3,6–10], cholesterol malabsorption and enhanced synthesis in the liver and in other tissues [11,12]. We previously demonstrated that CF bronchial epithelial cells accumulate lipids and exhibit a higher content of the sphingolipid ceramide, which is known to contribute to CF airways inflammation [13], together with glycerophospholipids and cholesterols [14,15]. Furthermore, we showed that de novo synthesis of sphingolipids is up-regulated in acute and chronic inflammation [16,17]. By modulating sphingolipid synthesis and impairing the accumulation of ceramide with Myriocin (Myr), we were able to reduce also glycerol- and cholesterol-based lipids [14,15], to promote fatty acids (FA) oxidation [14], to reduce inflammation and oxidative stress and to restore defensive response against pathogens infection, which is defective in CF [18–20].

Due to their hydrophobicity, intracellular lipids traffic is either vesicles or protein-mediated. Lipid Droplets (LDs) are ubiquitous organelles that function as a storage of intracellular lipids to regulate cellular lipid homeostasis. LDs biogenesis initiates at the endoplasmic reticulum (ER), by triacylglycerol (TAG) synthesis, followed by their nucleation and lens formation. Next, a budding process occurs, leading to an ER anchored droplet. In addition to incorporating newly synthesized lipids, LDs serve as a storage and reservoir of cellular lipids and take part in important processes such as the response to oxidative stress and autophagy induction during stress or nutrient depletion. LDs ensure the homeostasis of membranes, organelles, energy, and redox balances by sequestering toxic molecules, preventing lipid peroxidation, removing damaged proteins, and acting as a supply of key signaling lipids involved in inflammation and immunity [21,22]. Autophagy, another important stress defensive mechanism, supports LDs biogenesis, contributing to shifting their role from structural lipids pool towards energy-related lipid storages, which may finally be used via lipophagy and lysosomal acid lipolysis [23,24]. In addition, during autophagy, FA are sequestered in LDs to prevent the accumulation of acyl-carnitines, which would disrupt mitochondrial integrity [25]. Importantly, impaired chloride ions exchange was reported to reduce LDs size by downregulation of their fusion [26]. These observations suggest that CF proteinopathy can impair autophagy and hinder LDs biogenesis, causing lipid accumulation and the related exacerbation of inflammation,

Here, we compare the lipid distribution in CF and healthy bronchial epithelial cells to investigate a possible defective LD formation and related lipid metabolism. We hypothesize that Myr can restore lipid homeostasis in CF by reducing lipid content, promoting FA oxidation and inducing autophagy. We speculate that lipid metabolism regulation may be an innovative therapeutic approach in CF.

2. Materials and methods

2.1. Reagents and antibodies

The following materials were purchased: LHC Basal, LHC-8 w/o gentamicin culture media from Gibco (USA); Fetal Bovine Serum and Minimum Essential Medium Earle's salt from EuroClone Life Science (Italy); penicillin/streptomycin and RIPA buffer were purchased from Sigma-Aldrich (USA); OA/BSA cell culture mix (Sigma-Aldrich, USA); protease inhibitors cocktail (Roche, Switzerland); Quick Start™ Bradford Dye Reagent and Clarity™ Western ECL Blotting Substrates, iScript™ cDNA synthesis, retro-transcription kit (BioRad, Italy); BODIPY 493/503 (4,4-difluoro-1,3,5,7,8-pentamethyl-4-bora-3a,4a-diaza-s-indacene), catalogue number D3922, and BODIPY™ 558/568 C12 (4,4-Difluoro-5-(2-Thienyl)-4-Bora-3a,4a-Diaza-s-Indacene-3-Dodecanoic Acid), catalogue number D3835, Prolong® Gold antifade reagent, were purchased from ThermoFisher Scientific, Molecular Probes™ (USA); NE-PER™ Nuclear and Cytoplasmic Extraction Reagents from ThermoFisher Scientific (USA); ReliaPrep™ Miniprep RNA extraction System and GoTaq qPCR Master Mix (Promega, USA); SYBR Green (Takara, Japan); synthetic oligonucleotides from eurofins genomics (Germany). Primary antibodies: anti- PPAR-γ, anti-NRF2 and anti-Lamin A (ElabScience, USA), anti-SQSTM1/p62 (D1Q5S), anti β-ACTIN (Sigma-Aldrich, USA), anti-TFEB (ab2636, Abcam, UK). The secondary antibodies were purchased from Jackson Laboratories (Bar Harbor, ME, USA). Human MDA (Malondialdehyde) Elisa Kit was purchased from Fine Test, Labospace (Italy).

2.2. Cells and treatments

IB3-1 cells (named CF cells), an adeno-associated virus-transformed human bronchial epithelial cell line derived from a CF patient (ΔF508/W1282X) and provided by LGC Promochem (USA), were grown in LHC-8 medium supplemented with 10% FBS, 1% penicillin/streptomycin at 37 °C and 5% CO_2. Human lung broncho-epithelial cells 16HBE14o- (named healthy cells), originally developed by Dieter C. Gruenert, were provided by Luis J. Galietta, (TIGEM, Napoli) and cultured, as recommended, in Minimum Essential Medium (MEM) Earle's salt, supplemented with 10% FBS, 1% penicillin/streptomycin at 37 °C and 5% CO_2. When indicated, cells have been pretreated with oleic acid (OA) and bovine serum albumin (BSA) sterile solution (33 μM OA, 4 h, followed by additional 24 h either alone or in combination with Myr). Myr treatments (24 h) were performed at a concentration of 10 or 50 μM, in 100 mm dishes plated at 1×10^5 cells/each. At least triplicate samples for each experiment were performed, except differently indicated.

2.3. Lipidomic analysis

Lipids extraction from cell pellets (0.5-1 $\times$ 10^6 cells) was performed using a monophasic extraction method with water: chloroform: methanol (1:3:6 *v*/v/v). Purified extracts were analyzed by a Shimadzu UPLC coupled with a Triple Tof 6600 Sciex, running data-dependent acquisition with positive electrospray ionization. All samples were analyzed in duplicate for the identification and semi-quantification of lipids. The separation was achieved by an Acquity BEH C18 column 1.7 μm 2.1 $\times$ 100 mm (Waters, USA) using as mobile phase (A) water/acetonitrile (60:40) and as mobile phase (B) 2-propanol/acetonitrile (90:10) both containing 10 mM ammonium acetate and 0.1% of formic acid. The lipidomics data analysis was processed using MS-DIAL (ver. 3.4). Data analysis and plotting were achieved with MetaboAnalyst (ver. 4.0), after being log-transformed and auto-scaled [15].

2.4. Microscopy analysis

Cells were seeded on glass slides and grown for 24 h (70% confluence). For FA incorporation to label lipid biosynthesis, BODIPY™ 558/568 C12 was added to culture medium, according to manufacturer's instruction, and cells were labeled overnight. For neutral lipid staining, the BODIPY 493/503 was added to the culture medium, according to manufactures instruction, and cells were labeled for 30 min. Next, the slides were washed and dried for 3 min at room temperature, fixed in 4% buffered formalin for 30 min at RT, rinsed twice in PBS as previously shown [27]. Sections on a glass slide were inverted and mounted onto glass slides by means of anti-fading and DAPI containing mounting

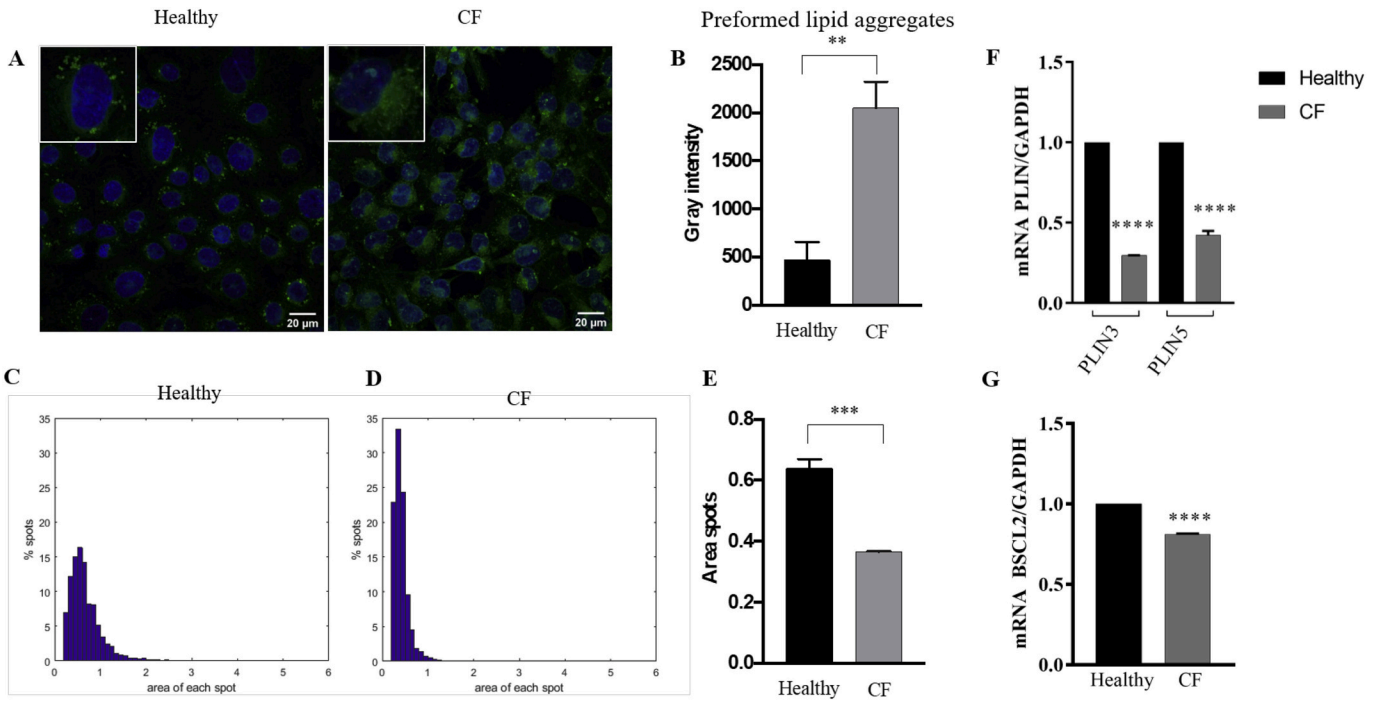

Fig. 1. Different intracellular lipid storage in CF and healthy epithelial cells in basal condition. (A) Confocal immunofluorescent images of CF and healthy cells and (B) histograms of mean fluorescence intensity (gray intensity). Images were obtained after staining of neutral lipid aggregates (Bodipy green) and nuclear counterstaining (DAPI blue), scale bars represent 20 μm. (C—D) Histograms representing the percentage of spots having a defined area (in μm^2) in the entire population of Healthy (C) and CF (D) cells analyzed, respectively. Bin width 0.1um^2. (E) Histograms of the medium value of spot's area (in μm^2) in CF and healthy cells. (F-G) Difference of lipid droplets genes expression in CF and healthy cells measured by qRT-PCR and represented as fold change of CF versus healthy cells. All data are expressed as mean ± SE (** $p < 0.01$; *** $p < 0.001$; ****$p < 0.0001$); two-tailed unpaired Student's *t*-test.

reagent for nuclei counterstaining. Confocal images were acquired using Nikon A1 Laser Scanning Confocal microscope (60× oil immersion objective). Image quantitation was performed using Fiji analysis software. All values were normalized onto nuclei count. For spot counting and quantification, cells were seeded in 24 wells plates and treated as above indicated. The plates were processed in full automation by using IN Cell Analyzer 1000, General Electric Co (now Cytiva). A Nikon Plan Fluor 40× (NA 0.6; 0,161 μm/pixel) dry objective was used to capture 25 images for each well. Dapi staining was detected with an excitation wavelength of 360 ± 40 and emission wavelength of 460 ± 40, while Bodipy green signal was detected with an excitation wavelength of 480 ± 40 and emission wavelength of 535 ± 50. Developer Toolbox software was used to count the green spots in cells and measure the area of every single spot. The experiment IN Cell Analyzer was performed once with triplicate samples.

2.5. ELISA kit

Levels of oxidative stress were measured using an MDA Elisa kit (Fine Test, Labospace, Italy) following the manufacturer's protocols. Briefly, cells were treated or not with Myr 50 μM for 24 h. Following treatments, the supernatant was collected and centrifuged at 1000 xg for 20 min at 2–8 °C, to remove insoluble impurity and cells debris. The supernatant was dispensed into the wells; 50 μl biotin-labeled antibody (included in kits) was added, and the plate was incubated at 37 °C for 45 min. The samples were washed three times with wash buffer before adding 100 μl HRP-Streptavidin Conjugate (SABC). The plate was incubated at 37 °C for 30 min. The wells were washed three times with wash buffer, followed by the addition of 90 μl of TMB substrate; the plate was incubated at 37 °C in the dark for 15–20 min. After adding the stop solution into each well, absorbance was measured at 450 nm using a microplate reader (EnSight™, PerkinElmer, USA).

2.6. Protein extraction and western blotting

For transcriptional factors, western blottings, nuclear and cytoplasmic protein extract from cells were obtained with the NE-PER Nuclear and Cytoplasmic Extraction Reagents kit (ThermoFisher Scientific, USA) according to the manufacturer's instructions. Total cell proteins were extracted from cells in RIPA buffer. The concentration of proteins in lysates was measured by Quick Start™ Bradford Dye Reagent (595 nm OD read). 20 μg of proteins *per* sample were separated on SDS-PAGE gel and electro-blotted onto a nitrocellulose membrane. After washing in Tris-buffered saline containing 0.1% Tween-20 (TBS-T) and blocking with 5% non-fat dry milk for 1 h at room temperature, membranes were probed overnight at 4 °C with the primary antibodies. After three washes in TBS-T, the blot was incubated with the horseradish peroxidase-conjugated secondary antibodies. After the final washings, proteins were detected using an enhanced chemo-luminescent horseradish peroxidase substrate, and the relative bands were captured and quantified by Alliance™ UVITEC Cambridge (UK).

2.7. RNA extraction and sequencing

Total RNA was isolated from harvested cells with the ReliaPrep™ Miniprep RNA extraction system (Promega, USA), according to the manufacturer's instructions.

Sequencing was performed on Illumina NextSeq using the protocol SMART-Seq for the preparation of the libraries, obtaining an average of 15 million single-end reads per sample. All sequences are of fixed length 75 bp, and have a high quality for a single base.

2.8. RNA-seq data analysis

Raw single-end reads were aligned to the human reference genome (GRCh38) using STAR [28] and only uniquely mapping reads were

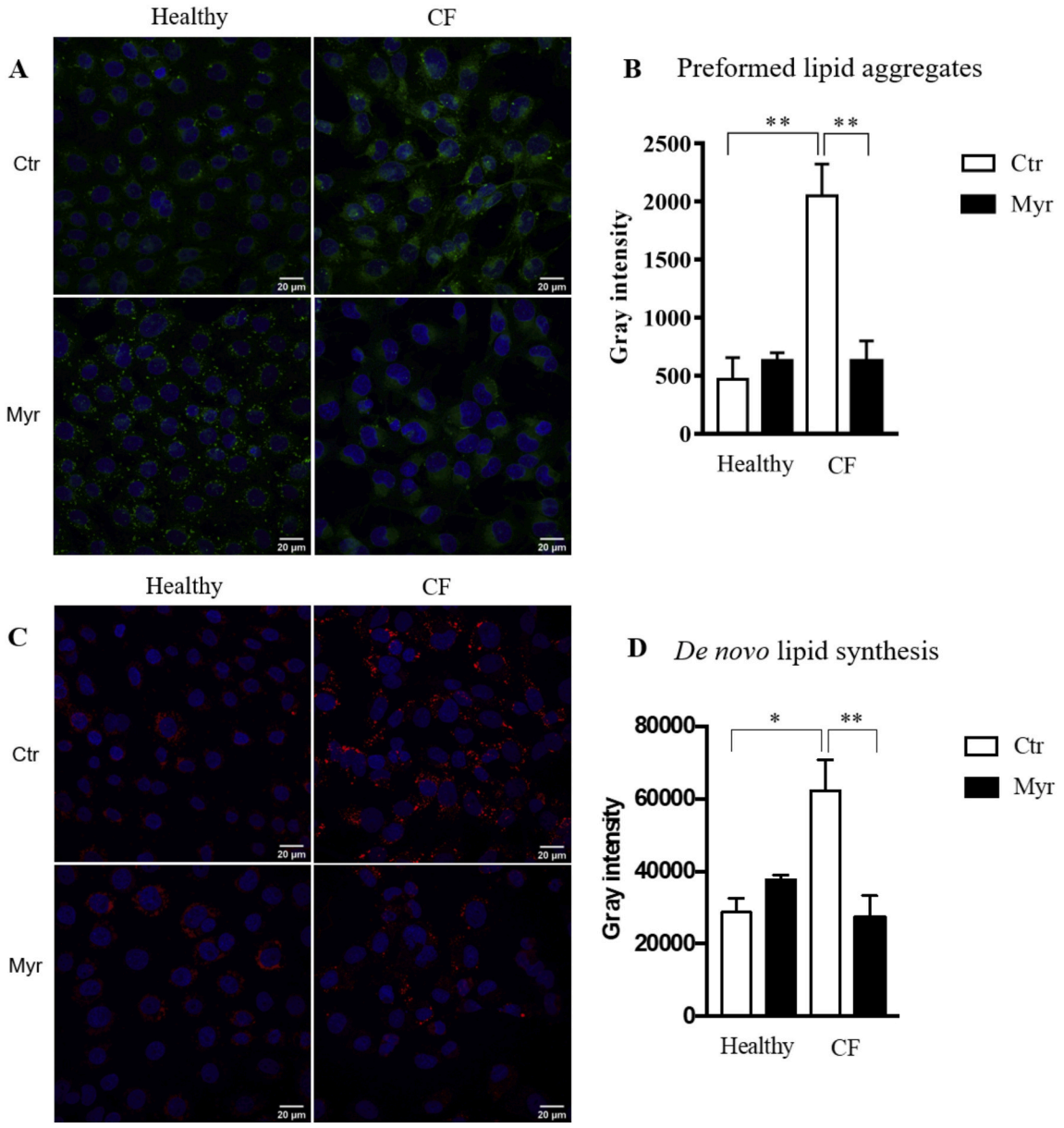

Fig. 2. Different Myr effects on intracellular lipid storage in CF and healthy epithelial cells. Confocal immunofluorescent images of CF cell line and healthy cell line, either treated or not with 50 μM Myr for 24 h. Confocal images were obtained after staining of neutral lipid aggregates (green, A) or by labeling de novo synthesized fatty acids containing lipids (red, C); DAPI (blue), nuclear counterstaining. Scale bars represent 20 μm. Representative histograms of intracellular lipids fluorescence (gray intensity) are shown (B and D). Data are presented as means ± SE (* $p < 0.05$; ** $p < 0.01$); one-way ANOVA test followed by Bonferroni correction was used for all data.

considered for downstream analyses. Reads were assigned to genes with featureCounts [29], using the gencode primary assembly v.31 gene transfer file (GTF) as a reference annotation file for genomic features boundaries. Raw counts matrices were then processed with the Deseq2 package [30] following the standard workflow. In particular, we evaluate both in CTRL and CF cells the effect of Myr comparing treated versus untreated condition. Genes with FDR less than 0.05 were considered differentially expressed (DEGs; in Fig. 7A, ACADSB and ACADVL were added in the list despite their p.adj was slightly higher than 0.05 threshold). Downstream analysis, including Gene Set Enrichment Analysis (GSEA) and Over Representation Analysis (ORA) were performed with ClusterProfiler Bioconductor package [31] using a list of databases including Gene Ontology (GO), Kyoto Encyclopedia of Genes and Genomes (KEGG), Reactome pathway and the Molecular Signatures Database (MsigDB). Enriched terms with a q-value <0.05 were considered statistically significant. Charts and images were produced using ggplot2 R package.

2.9. qRT-PCR

1 μg of purified RNA was reverse-transcribed to cDNA. The amplification was performed for the following target genes: CPT1A, SREBF1, NRF1, IL-β, TBK1, TP53INP, TMEM59, PPARα, NPC1, NPC2, SNX14, FITM2, BSCL2, PLIN2, PLIN3, and PLIN5. Relative mRNA expression of target genes was normalized to the endogenous GAPDH control gene and represented as fold change versus control, calculated by the comparative CT method (ΔΔCT Method). The analysis was performed by referring to control values that do not significantly differentiate (triplicate samples, and their standard deviation value divided by their mean value is <1) [32]. Real-time PCR was performed by SYBR Premix Ex

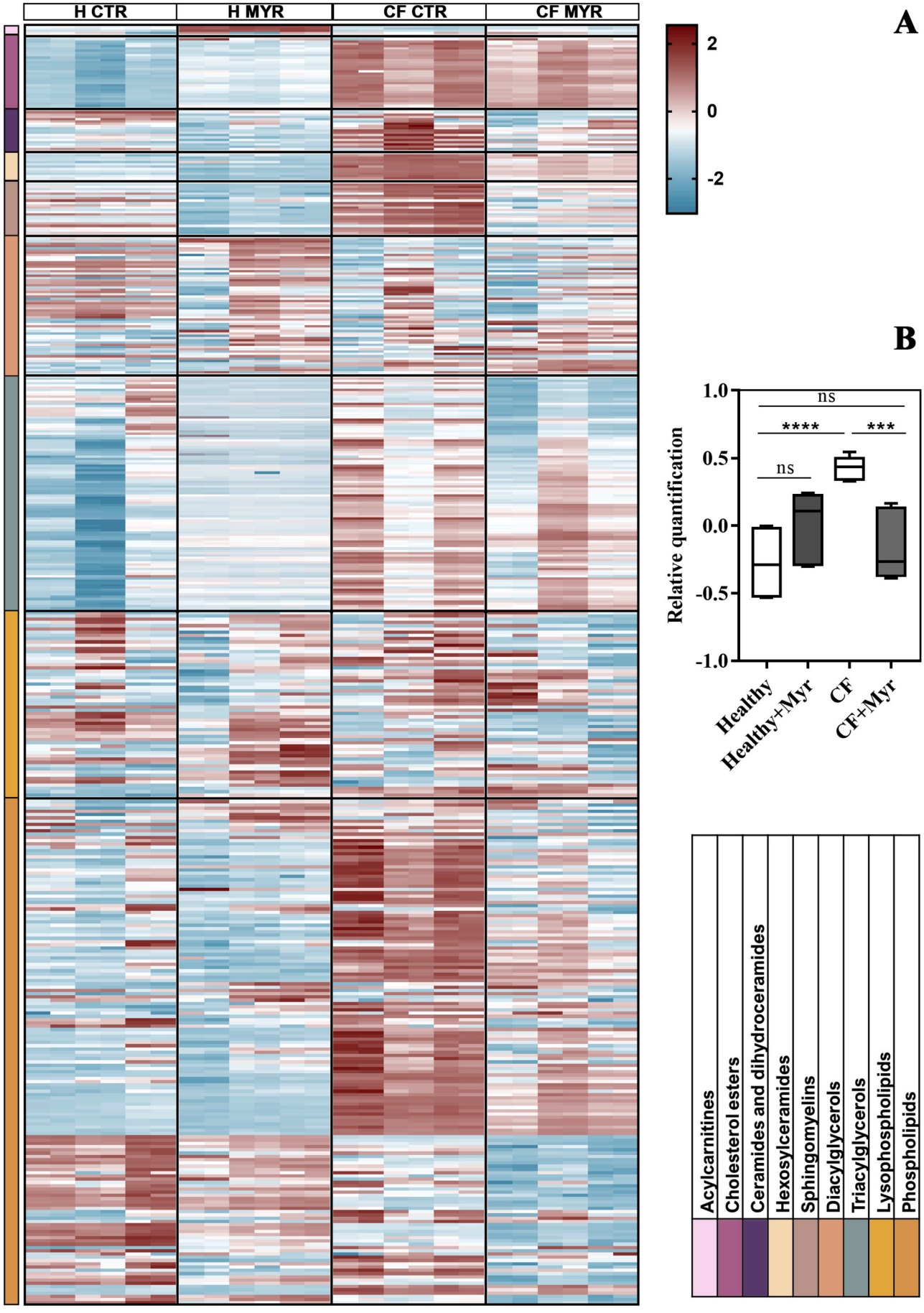

(caption on next page)

Fig. 3. A) Heatmap of the entire lipidome ($n = 625$ species) in different cell phenotypes treated or not with Myriocin, divided in columns. Features, in rows, were log-transformed and auto-scaled for visualization. The color-scale differentiates values as high (red), mid (white), and low (blue). The left color-scale indicates the different lipid classes. (B) Relative quantification of all the lipids identified in cell pellets (n = 6 for each class). Boxplots are defined with the first and third quartiles (25th and 75th percentile) for lower and upper hinges, min-max for the length of the whiskers, and median for the centerline. Statistical significance was investigated by unpaired one-way ANOVA with Bonferroni post-hoc test.

Taq™ II (Takara, Japan); primer sequences for SNX14 and NPC1, NPC2 was previously published [33,34]; all other sequences are available on request.

2.10. Statistical analysis

Data are expressed as mean ± SE, calculated from experimental replicates. The normal distribution of the data was checked by the Kolmogorov-Smirnov test. Data significance was then evaluated by one-way ANOVA test followed by Bonferroni correction ($p < 0.05$) or two-tailed Student *t*-test, as specified in figure legends. Statistical analysis was performed by GraphPad Instat software and graph illustrations generated by GraphPad Prism software (La Jolla, USA).

3. Results

3.1. Differential lipid distribution in CF cells compared to healthy cells

In order to verify the defect of lipid metabolism in CF cells, we labeled the cells by means of a fluorescent probe with a high affinity for neutral lipids. We compared CF to healthy cells. A slight but consistent increase of the fluorescence signal (Fig. 1 A and B) demonstrates a higher overall accumulation of lipids in CF compared to healthy cells. We observed a different signal intensity and a different lipid distribution, which appears as lipid aggregates, organized in intracellular structures in healthy cells (resembling lipid droplets) and conversely widespread in CF cells, that exhibit more diffused fluorescence. To confirm the data, we analyzed each fluorescence spot area, observing that the percentage of large spots is higher in healthy cells than in CF cells (Fig. 1 C—D). Furthermore, the average of spots' area was significantly higher in healthy than CF cells (Fig. 1 E). In order to identify the role of lipid aggregates, we evaluated the association between the presence of lipid structures and the expression of LDs markers as perilipins (PLINs) and seipin (BSCL2). We observed a reduction in the expression of PLIN3, PLIN5 and BSCL2 in CF cells compared to healthy cells (Fig. 1 F and G). These data suggest that the CF cells exhibit an accumulation of widespread lipids and a reduced ability to form lipid droplets.

In order to understand the role of Myr in lipid mobilization and catabolism, we labeled neutral lipids in Myr-treated CF and healthy cells and observed that Myr was able to significantly reduce lipids in CF but not in control cells (Fig. 2A and B). Here, we investigated the effects of Myr on FA containing lipids synthesis. To this purpose, we labeled cells with a fluorescent FA (lauric acid), which is incorporated in FA containing lipids (Fig. 2C and D) and quantified the fluorescence per cell. First, we observed an increased amount of new synthesized FA

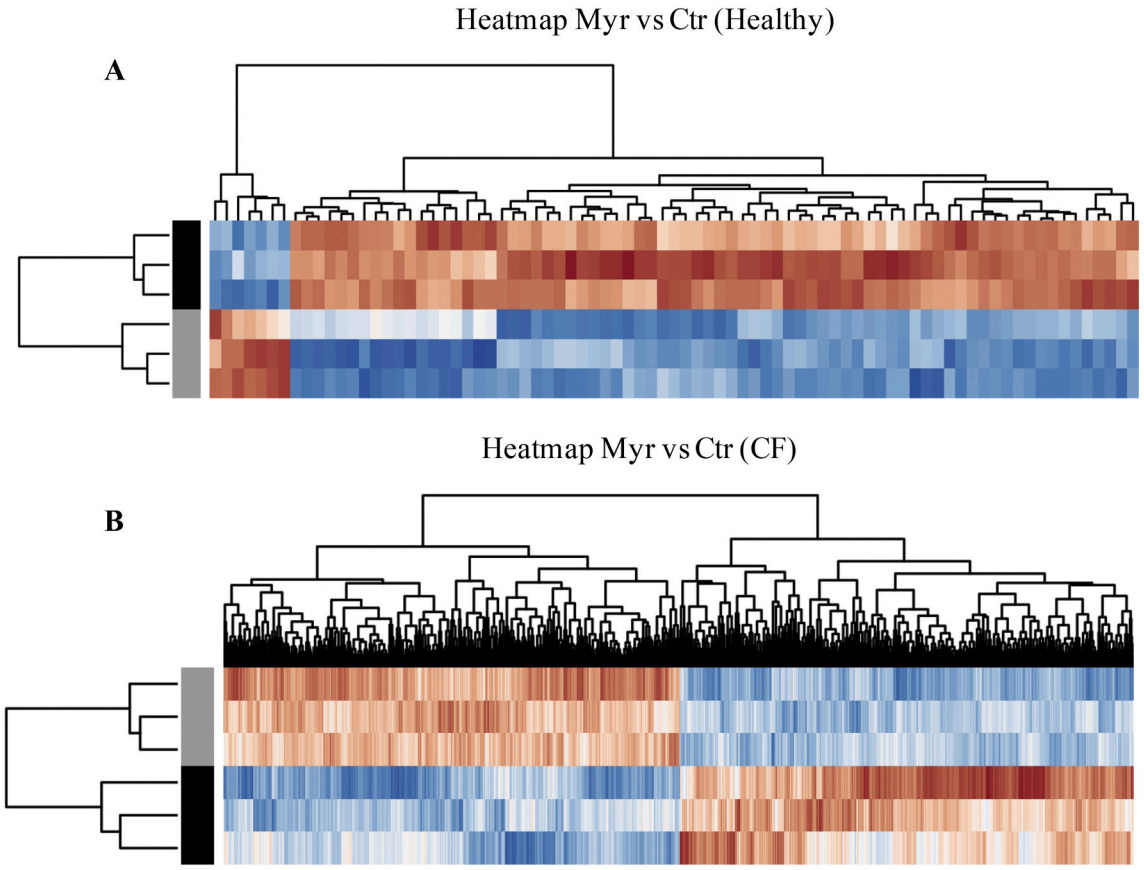

Fig. 4. Myr (10uM Myr for 24 h) effect on gene expression profile in CF and healthy cells. RNAseq analyses. Heatmap of DEGs obtained from the comparison of treated and untreated conditions both in healthy (A) and CF cells (B). In the chart are shown the row-scaled gene expression rlog values. Tiles are colored according to up (red) or down (blue) regulation. In black the untreated samples, whereas in gray the Myr-treated samples. Chart produced with ggplot2.

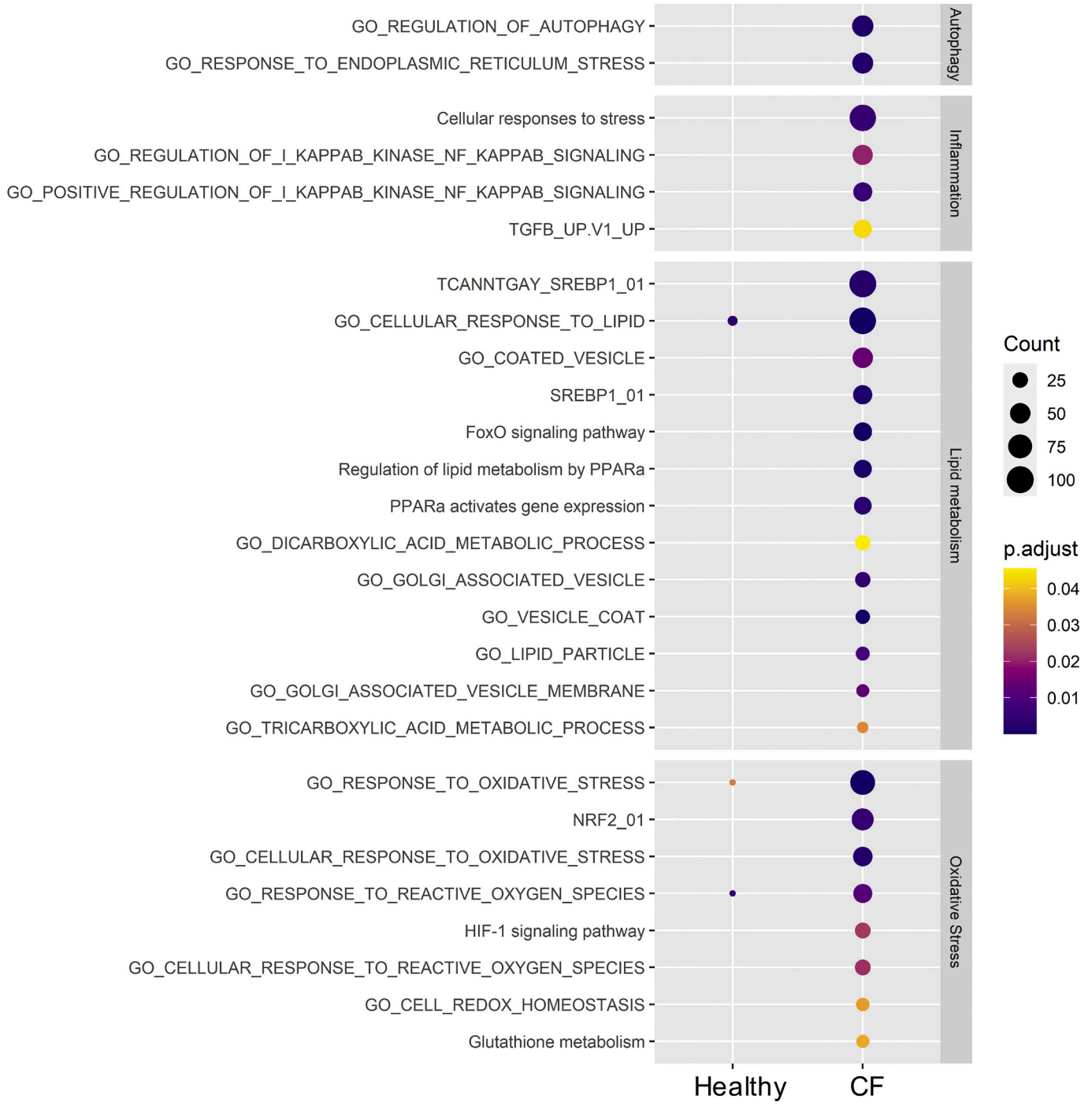

Fig. 5. Dotplot of enriched terms related to CF, comparison between CF and Healthy cell lines. The plot shows enriched terms observed in CF grouped by custom categories. Very few terms resulted enriched in the Healthy cell line. Size of the dot describes the number of DEGs belonging to the enriched terms, whereas the color represents the p-adjust value from the Over-Representation test.

containing lipids in CF compared to healthy cells. Second, we demonstrated that Myr treatment induced a significant reduction of fluorescence in CF cells. The above-reported data suggest that Myr effects could be mediated by its ability to restrain lipid synthesis, enhancing, at the same time, their catabolism and oxidation.

3.2. CF and healthy epithelial cell lines exhibit a different lipidomic and transcriptional profile in response to sphingolipid synthesis inhibition

We investigated the effect of Myr on total lipid molecules in healthy and CF cells by untargeted LC/MS and observed a different pattern of lipids, with CF cells displaying a diffused accumulation in lipids that can be partially counterbalanced by Myr treatment (Fig. 3A). Specifically, we observed that sphingolipids (ceramides, hexosylceramides, dihydroceramides, sphingomyelins) are significantly increased in CF cells and reduced by Myr treatment. A similar behavior is shown for lipids involved in energy metabolism (such as triacylglycerols) and in structural or signaling roles such as phospholipids and lyso-phospholipids and in cholesterol esters. A significant decrease in acyl-carinitine, partially corrected by Myr treatment, is found in CF compared to control cells. The semi-quantitative analysis showed that an increase in total lipids amount characterize CF cells compared to healthy cells and Myr

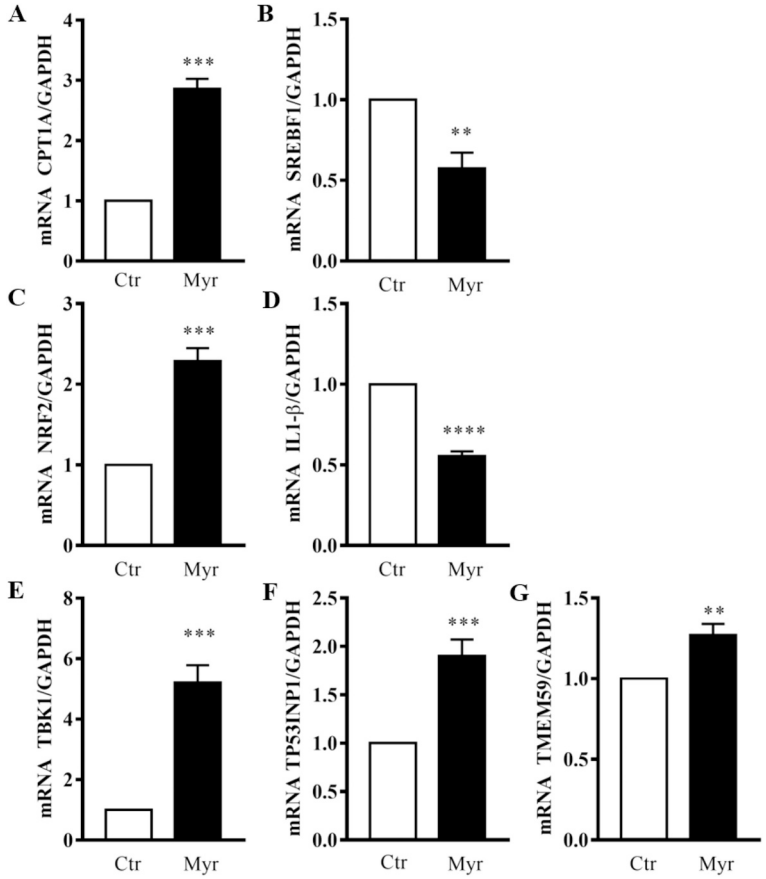

Fig. 6. RNA-seq validation by RT-PCR quantification of the expression of genes involved in lipid metabolism (A,B); oxidative stress and inflammation (C,D); autophagy (*E*-G). GAPDH was used as a housekeeping gene. Data, derived for triplicate samples, are expressed as mean ± SE (** $p < 0.01$; *** $p < 0.001$; **** $p < 0.0001$); two-tailed unpaired Student's *t*-test.

treatment significantly reduces it (Fig. 3B).

In order to better understand the therapeutic effect of sphingolipid synthesis inhibition in CF, we analyzed the transcriptomic profile of CF and healthy cells. We performed an RNA-sequencing analysis of CF and healthy epithelial cells after Myr treatment for 24 h. As shown in Fig. 3, Myr induced a stronger modification of the transcriptional profile in CF cells than in healthy cells, as shown by the higher number of annotation bars in CF cells than in healthy cells. Furthermore, the different red (up) and blue (down) color distribution shows a different amount of up and down-regulated genes in the two cell lines. We identified only 55 Differentially Expressed Gene (DEGs) in healthy cells and 1629 DEGs in CF cells in response to Myr treatment (Fig. 4).

3.3. Myriocin modulates gene sets involved in autophagy, lipid metabolism, inflammation and oxidative stress in CF cells

Next, we investigated the Myr-modulated genes in CF cells. Starting from the DEG list, over-representation analysis was performed using different gene sets (GO, KEGG, MSigDB), in order to identify the presence of enriched functional categories. In particular, categories related to CF disease, such as autophagy, lipid metabolism, inflammation and oxidative stress, were identified (Fig. 5). We strikingly noticed that whereas in control cells, very few genes belonging to these major ontologies were modulated by Myr, an elevated number of genes were significantly modulated in CF cells among the above-mentioned clusters.

To validate these findings, the expression of a few genes representative of each category identified by enrichment analysis was evaluated

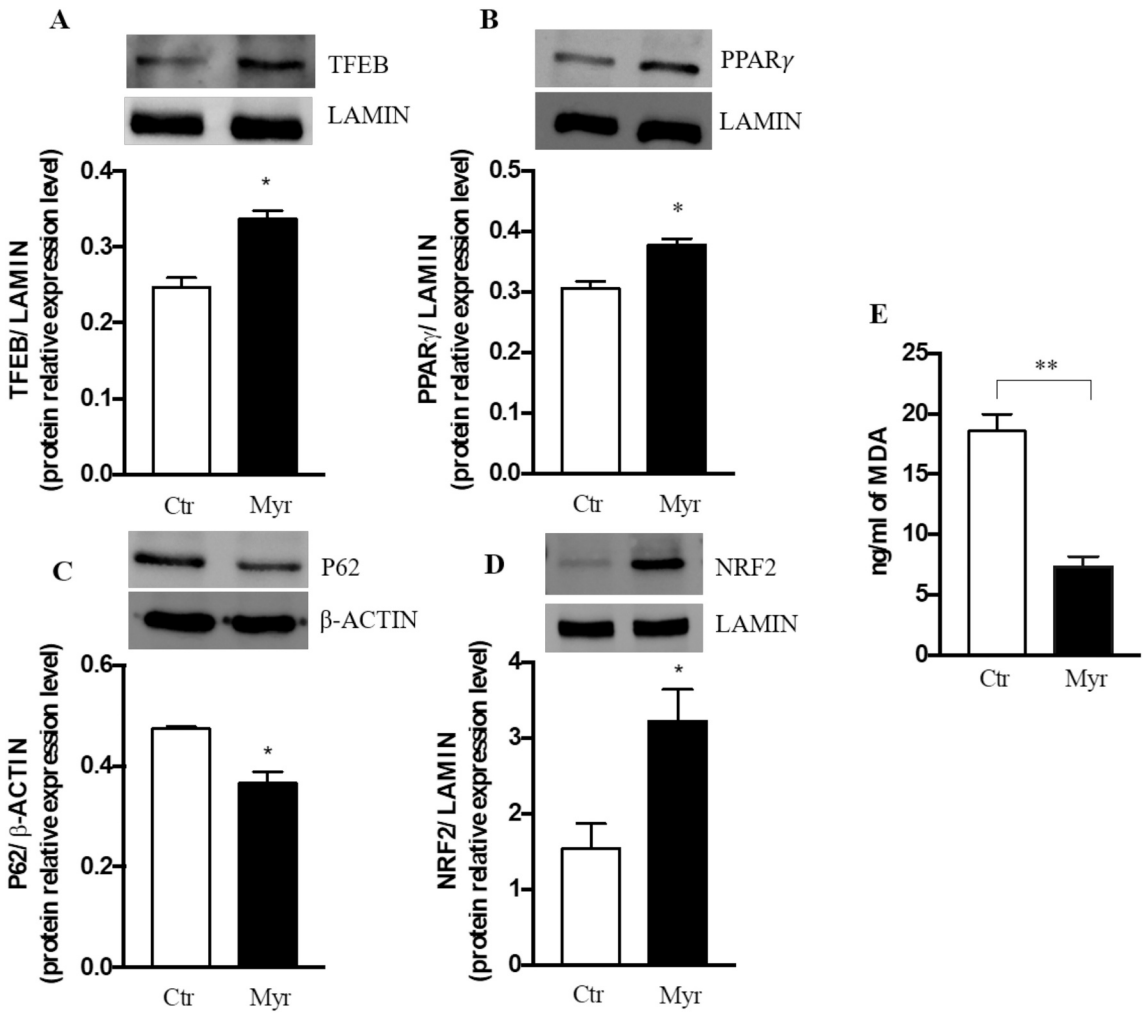

Fig. 7. Myr effect on oxidative stress by modulating lipid metabolism (24 h treatment) (A-C) Measurement of nuclear translocation of TFEB, PPARγ and NRF2 by western blot analysis on nuclear extracts, normalized on LAMIN A. (D) Quantification of P62 protein expression by western blot analysis on whole lysates and normalized on β-ACTIN. Protein signals were quantified by densitometric analysis. (E) Measurement of lipid peroxidation in CF cells treated with Myr by MDA Elisa kit. All data are expressed as mean ± SE (* $p < 0.05$; ** $p < 0.01$); two-tailed unpaired Student's *t*-test.

by RT-PCR (Fig. 6A-G). The obtained data showed that Myr increased the carnitine palmitoyl transferase 1a (CPT1A) expression and inhibited the sterol regulatory element binding transcription factor 1 (SREBF1) expression, two genes belonging to the category of lipid metabolism (Figs. 6A and B). Regarding the ontologies of oxidative stress and inflammation, we observed an increase of the Nuclear Factor Erythroid 2 (NFE2L2/NRF2) and a decrease of Interleukin 1 β (IL-1β) gene expression in Myr-treated CF cells (Figs. 6C and D). Finally, we found that Myr increased the expression of TANK Binding Kinase 1 (TBK1), Tumor Protein P53 Inducible Nuclear Protein 1 (TP53INP1) and Transmembrane protein 59 (TMEM59) genes involved in autophagy processes (Fig. 6E, F and G).

3.4. *Myr activates transcription factor EB (TFEB) mediated response to stress*

We previously demonstrated that, by reducing lipid synthesis, Myr activates an early TFEB-induced response to stress (5 h) [14]. TFEB controls lipid metabolism, inflammation, and oxidative stress by activating peroxisome proliferator-activated receptors (PPARs) and by autophagy induction. We here demonstrated that Myr induces a sustained TFEB nuclear migration (up to 24 h), together with PPARγ (figure7A and B) and concomitantly to the activation of oxidative stress response via autophagy-mediated clearance of p62 (Fig. 7C), allowing the release of an active NRF2. We found that Myr induced nuclear migration of NRF2 (Fig. 7D). Indeed, these events lead to reduced lipid peroxides products (Fig. 7E).

3.5. *Myr transcriptionally regulates genes involved in lipid consumption and droplets formation*

Through the analysis of the DEGs between Myr-treated and untreated CF cells, we selected the key genes involved in lipid consumption and lipid droplets formation. Fig. 8 shows the top genes involved in lipid metabolism, lipid traffic, oxidation, remodeling and droplets formation, that were up- or down-regulated by Myr treatment. Myr up-regulated the expression of: PPARα that regulates lipid metabolism, TAG remodeling enzymes such as glycerol-3-phosphate acyl transferase 3/4 (GPAT 3/4), lipase A (LIP A) for cholesterol esters formation, Niemann-Pick C proteins (NPC 1 and 2) for intracellular cholesterol transport. Moreover, Myr up-regulated genes encoding proteins that are localized at ER–LD contact sites and involved in the maturation/growth process of LDs biogenesis, such as: sorting nexin 14 (SNX 14); fat storage inducing transmembrane protein 2 (FITM 2); abhydrolase domain containing proteins (ABHD2 and ABHD3), whose family members have been reported to interact with PLINs in the promotion of triglycerides mobilization from LDs storages [35]. In addition, the transcription of CPT2 (carnitine palmitoyl transferase 2), CROT (carnitine O-octanoyl

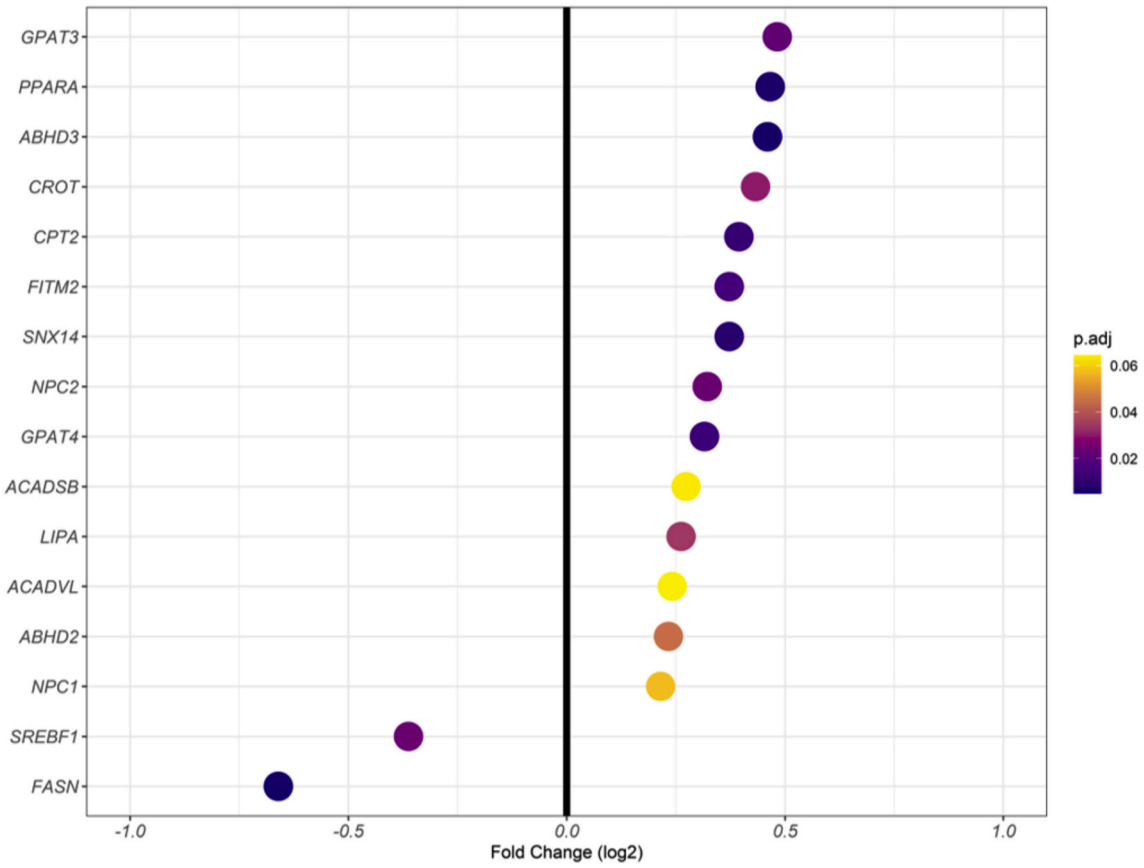

Fig. 8. Dotplot of DEGs involved in lipid consume and lipid droplets formation. On the x-axis the fold changes (log2), dots are colored according to the p.adj value from Myr-treated vs untreated CF test. Chart produced with ggplot2.

transferase) and acyl-CoA dehydrogenase (ACAD), regulating FA mitochondria entry and their oxidation, was also increased. In line with promoting lipid traffic, storage or oxidation, Myr downregulated SREBF1, which drives cholesterol and other lipid synthesis and FASN, fatty acid synthase.

As Myr is known to reduce the excess of cytosolic lipids in CF cells by transcriptional regulation of genes involved in lipid metabolism, we treated CF cells with oleic acid (OA/BSA) in order to enhance the FA cells load and investigated the expression of lipid droplets related genes under Myr treatment. Even in these conditions, Myr significantly increased the expression of PPARα, NPC 1 and 2, SNX 14, FITM 2. In addition, we observed a significant increase of the expression of PLIN2, 3 and 5 and of BSCL2 (Fig. 9). Importantly, PLIN 3 and 5 are downregulated in CF cells in comparison to healthy (Fig. 1).

4. Discussion

The present data demonstrate that lipid metabolism and organization is altered in CF. In agreement with the literature data reporting peripheral tissues accumulation of lipids in CF, we previously demonstrated that CF bronchial epithelial cells are enriched in most of the structural lipids species, compared to normal cells [14,15]. We also demonstrated that induction of FA oxidation in CF cells restores the defective autophagy and pathogen killing [14,20], pointing out a possible deficiency of lipid catabolism at the root of autophagy impairment. Since we already proved that sphingolipid synthesis is enhanced in CF, we studied the formation of other lipids by labeling cells with lauric acid and following FA incorporation into complex molecules (red fluorescence). To note, we showed an increased acyl-containing lipids synthesis in CF compared to healthy cells, suggesting that not only lipid catabolism is affected by proteinopathy but also their biosynthesis. Another relevant difference observed in CF cells is their lipids differential distribution within the cytosol, with organized structures resembling LDs in healthy cells and markedly diffused lipid signal in CF (green fluorescence). This is flanked by a reduced expression of PLINs, which correlates with the defective size of LDs in chloride transport deficient cells [26]. Other than being involved in LDs biogenesis, PLINs take part in their maturation process. PLINs reduced expression in CF may contribute to lipid altered distribution. We also observed a marked reduction in the expression of seipin (BSCL2), an ER membrane protein that exerts an important role in the conversion of nascent to mature lipid droplets by transfer of lipids [36,37]. Since Myr exerts a defensive response against stress, via autophagy induction and energy production from FA oxidation [14], here we demonstrated that Myr reduces overall lipids content (green fluorescence) and significantly reduces the synthesis of acyl-containing lipids (red fluorescence), the expression of the lipid synthesis key promoter SREBPF1 and other genes involved in the pathway, such as FASN. A semi-quantitative analysis confirms that CF cells exhibit an increased content of most lipid classes analyzed. Ceramides are significantly enhanced in CF versus healthy cells and reduced upon Myr treatment, in agreement with our previous findings [19]. Interestingly, the fatty acids containing triacylglycerols and phospholipids exhibit a similar trend, in agreement with recently published lipidomic data on CF patients serum analysis [5]. The marked reduction of acyl-carnitine in CF cells may be associated with reduced fatty acid import for their oxidation. Myr treatment slightly increased this lipid class in CF cells. Myr treatment reduced the overall CF lipids content. The lung cells may sense the alteration of vesicles/lipid traffic, which is caused by the CF proteinopathy, and, therefore, promote the synthesis of lipids, with subsequent accumulation, LDs storage and

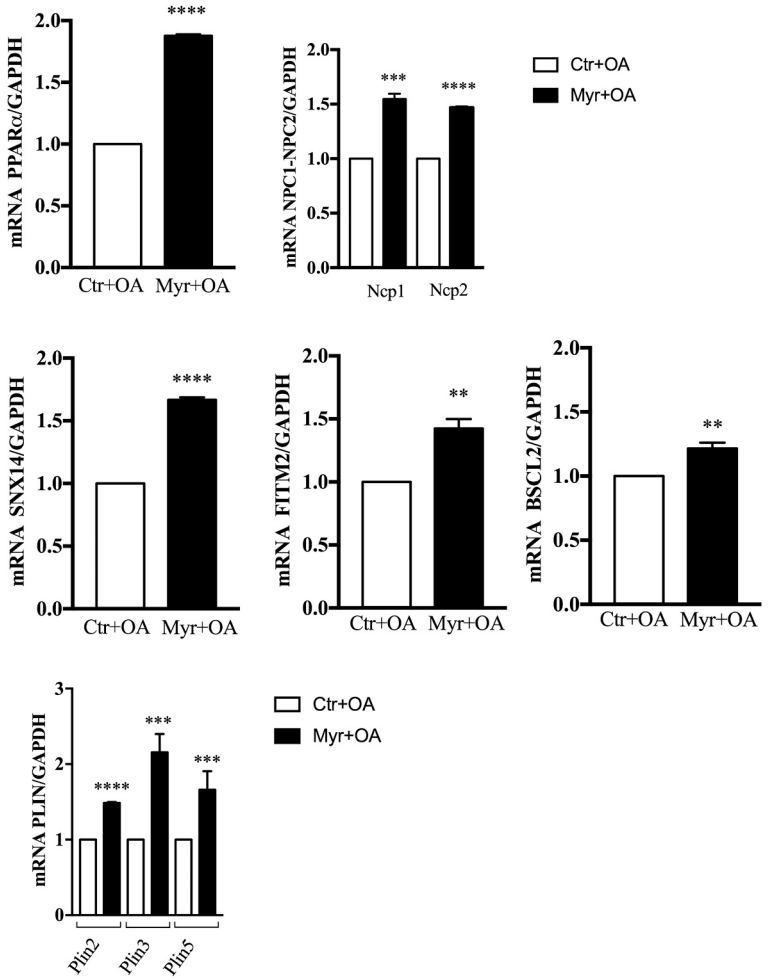

Fig. 9. Quantification of LDs marker genes by RT-PCR in CF cells after OA pretreatment (33 μM for 4 h) and subsequent Myr treatment (50 μM for 24 h). GAPDH was used as a housekeeping gene. Data, derived for triplicate samples, are expressed as mean ± SE (** $p < 0.01$; *** $p < 0.001$; **** $p < 0.0001$); two-tailed unpaired Student's *t*-test.

catabolism. This stack could be responsible for the rise of a vicious inflammatory cycle. To evaluate the mechanism of action and the therapeutic potential of Myr, we investigated gene expression profile under Myr treatment in both healthy and CF cells and observed that the number of modulated genes is significantly higher in diseased cells. This is in line with our previous observation that even if Myr targets the rate-limiting step of de novo sphingolipids synthesis, its administration significantly reduces total lipids in CF cells and modestly affects healthy cells [14,15,20]. Such enhanced sensitivity to Myr (at the low doses experimented) is possibly caused by an increased sphingolipid synthesis, which is related to CF lipid dysmetabolism and targeted explicitly by the molecule. Interestingly, we confirmed that Myr induces a sustained activation of TFEB, a master activator of autophagy and lipid catabolism, and PPARγ, which regulates lipid consumption and storage and inflammatory responses. Moreover, Myr, possibly via autophagy-related p62 clearance, activates NRF2, which promotes anti-oxidant response

and therefore reduces lipid peroxidation. This metabolic shift aim at stress defense leads to a transcriptional phenotype change. In agreement, RNAseq downstream analysis (ORA) highlighted DEGs belonging to key functional categories as inflammation (including IL1β), autophagy (including TBK1, TP53, TMEM59), oxidative stress (including NRF2), and lipid metabolism (including CPT1a and SREBF1). These two latter genes belong to "PPARα activates gene expression" and "regulation of lipid metabolism by PPARα" reactome terms, which also contain Nuclear Receptor Coactivator (NCO) and Mediator complex (MED) gene families. These two gene families are known as transcriptional coactivators and both enhance PPARs transcription and the regulation of FA peroxisomal and mitochondria oxidation [38–42]. NCOs and MEDs family members, were up-regulated by Myr. In addition, among all differentially expressed genes regulating lipid metabolism, Myr treatment of CF cells up-regulated: CPT1 and 2, ACADSB and ACADVL take part in FA oxidation; CROT and GPTA3/4 in glycerol lipids remodeling enzymes; NPC1, NPC2 [43,44] and LIPA respectively contribute to cholesterol transport and are directly involved in esterification; SNX14 and FITM2 code for proteins localized at ER–LD contact sites and directly involved in LDs biogenesis [45,46]; moreover SNX14 is also reported to promote autophagy process [33,47,48].

The overall data assess that lipid synthesis is increased in CF, whereas their catabolism is reduced, contributing to inflammation, oxidative stress and impaired autophagy. Interestingly, ontologies related to autophagy induction, stress response and inflammation and lipid metabolism were similarly regulated by Myr in CF patients derived monocytes, infected in vitro with *A. fumigatus*, in association with a slight but consistent improvement of infection clearance ability [20]. Not only do lipids accumulate, but also their traffic and subcellular storage in lipid droplets are affected. At the aim of validating the therapeutic potential of Myr, we stressed CF cells by feeding with oleic acid and evaluated the transcriptional effect of Myr on genes that are required for lipid droplets biogenesis, which is putatively defective [26]. Even under FA overload, Myr significantly increased (1) the expression of the lipid catabolism regulator PPARα, which is a crucial promoter of lipid droplets formation, (2) NPC1 and − 2 that mediate the lysosomal extraction and cytosolic transfer of cholesterol, (3) LDs related protein BSCL2, SNX14, FITM2 and PLIN2, −3, and − 5 that are specifically involved in lipid remodeling inward and outward of lipid droplets.

Interestingly, the expression of PLIN5 promotes both triglyceride storage and FA oxidation. PLIN5 expression is up-regulated by PPARs that promote the expression of genes involved in FA oxidation [49–51]. Lipid droplets stem at the ER, as small lens budding from ER membranes with the help of specific proteins [52]. Therefore, the budding process and transcriptional regulation may be regulated by Myr. We can hypothesize that Myr may favor the budding process by reducing sphingoid base formation at the cytosolic face of the ER. This hypothesis requires further investigation. On the other side, Myr induced up-regulation of both PLIN family and PPAR family members, suggesting that Myr promotes a transcriptional program that shifts cell metabolism from lipid accumulation to oxidation, intending to overcome lipo-inflammation.

5. Conclusion

Our data suggest that CF proteinopathy causes an impaired ability to use lipids for energy production and storage. Lipid droplets management could be disassembled, causing a vicious cycle of reduced lipid oxidation, storage and enhanced synthesis in peripheral tissues, significantly contributing to chronic inflammation. In this view, dyslipidemia should be considered a contributor to CF airways chronic damage, and thus lipid metabolism should become an important pharmacological and therapeutic target.

Funding

This research was funded by the Italian Cystic Fibrosis Foundation, Grant FFC#11–2016.

Declaration of Competing Interest

The authors declare no conflict of interest.

Acknowledgments

We thank the Italian Cystic Fibrosis Research Foundation for the financial support of this work. Dr. Michele Dei Cas was supported by the PhD program in Molecular and Translational Medicine of the University of Milan, Italy. We thank Fondazione Umberto Veronesi for supporting Dr. Francesca Pivari and Dr. Aida Zulueta with Post-Doctoral Fellowships 2020. Part of this work was carried out in OMICs, an advanced mass spectrometry platform established by the University of Milan. Part of this work was carried out at UNITECH NOLIMITS, an advanced imaging facility established by the University of Milan.

References

[1] J.S. Elborn, Cystic fibrosis, Lancet 388 (2016) 2519–2531.
[2] A. Luciani, V.R. Villella, S. Esposito, N. Brunetti-Pierri, D.L. Medina, C. Settembre, M. Gavina, V. Raia, A. Ballabio, L. Maiuri, Cystic fibrosis: a disorder with defective autophagy, Autophagy 7 (2011) 104–106.
[3] R.T. Tham, H.G. Heyerman, T.H. Falke, A.H. Zwinderman, J.L. Bloem, W. Bakker, C.B. Lamers, Cystic fibrosis: MR imaging of the pancreas, Radiology 179 (1991) 183–186.
[4] V. Figueroa, C. Milla, E.J. Parks, S.J. Schwarzenberg, A. Moran, Abnormal lipid concentrations in cystic fibrosis, Am. J. Clin. Nutr. 75 (2002) 1005–1011.
[5] A. Zardini Buzatto, M. Abdel Jabar, I. Nizami, M. Dasouki, L. Li, A.M. Abdel Rahman, Lipidome Alterations Induced by Cystic Fibrosis, CFTR Mutation, and Lung Function, J. Proteome Res. 20 (1) (2021) 549–564. Jan 1.
[6] T. Khoury, A.W. Asombang, T.M. Berzin, J. Cohen, D.K. Pleskow, M. Mizrahi, The clinical implications of fatty pancreas: a concise review, Dig. Dis. Sci. 62 (2017) 2658–2667.
[7] A. Chryssostalis, D. Hubert, J. Coste, R. Kanaan, P.R. Burgel, N. Desmazes-Dufeu, O. Soubrane, D. Dusser, P. Sogni, Liver disease in adult patients with cystic fibrosis: a frequent and independent prognostic factor associated with death or lung transplantation, J. Hepatol. 55 (2011) 1377–1382.
[8] M. Wilschanski, P.R. Durie, Patterns of GI disease in adulthood associated with mutations in the CFTR gene, Gut 56 (2007) 1153–1163.
[9] N.M. White, D. Jiang, J.D. Burgess, I.R. Bederman, S.F. Previs, T.J. Kelley, Altered cholesterol homeostasis in cultured and in vivo models of cystic fibrosis, Am. J. Physiol. Lung Cell. Mol. Physiol. 292 (2007) L476–L486.
[10] D.S. Hardin, A. LeBlanc, L. Para, D.K. Seilheimer, Hepatic insulin resistance and defects in substrate utilization in cystic fibrosis, Diabetes 48 (1999) 1082–1087.
[11] M. Gelzo, C. Sica, A. Elce, A. Dello Russo, P. Iacotucci, V. Carnovale, V. Raia, D. Salvatore, G. Corso, G. Castaldo, Reduced absorption and enhanced synthesis of cholesterol in patients with cystic fibrosis: a preliminary study of plasma sterols, Clin. Chem. Lab. Med. 54 (2016) 1461–1466.
[12] W.L. Ernst, K. Shome, C.C. Wu, X. Gong, R.A. Frizzell, M. Aridor, VAMP-associated proteins (VAP) as receptors that couple cystic fibrosis transmembrane conductance regulator (CFTR) Proteostasis with lipid homeostasis, J. Biol. Chem. 291 (2016) 5206–5220.
[13] V. Teichgraber, M. Ulrich, N. Endlich, J. Riethmuller, B. Wilker, C.C. De Oliveira-Munding, A.M. van Heeckeren, M.L. Barr, G. von Kurthy, K.W. Schmid, M. Weller, B. Tummler, F. Lang, H. Grassme, G. Doring, E. Gulbins, Ceramide accumulation mediates inflammation, cell death and infection susceptibility in cystic fibrosis, Nat. Med. 14 (2008) 382–391.
[14] A. Mingione, M. Dei Cas, F. Bonezzi, A. Caretti, M. Piccoli, L. Anastasia, R. Ghidoni, R. Paroni, P. Signorelli, Inhibition of sphingolipid synthesis as a phenotype-modifying therapy in cystic fibrosis, Cellular Physiol. and Biochem. 54 (2020) 110–125.
[15] M. Dei Cas, A. Zulueta, A. Mingione, A. Caretti, R. Ghidoni, P. Signorelli, R. Paroni, An innovative Lipidomic workflow to investigate the lipid profile in a cystic fibrosis cell line, Cells 9 (2020).
[16] M.R. Reforgiato, G. Milano, G. Fabrias, J. Casas, P. Gasco, R. Paroni, M. Samaja, R. Ghidoni, A. Caretti, P. Signorelli, Inhibition of ceramide de novo synthesis as a postischemic strategy to reduce myocardial reperfusion injury, Basic Res. Cardiol. 111 (2016) 12.
[17] P. Signorelli, L. Avagliano, M.R. Reforgiato, N. Toppi, J. Casas, G. Fabrias, A. M. Marconi, R. Ghidoni, A. Caretti, De novo ceramide synthesis is involved in acute inflammation during labor, Biol. Chem. 397 (2016) 147–155.
[18] K.A. Becker, H. Grassme, Y. Zhang, E. Gulbins, Ceramide in Pseudomonas aeruginosa infections and cystic fibrosis, Cellular Physiol. and Biochem. 26 (2010) 57–66.

[19] A. Caretti, A. Bragonzi, M. Facchini, I. De Fino, C. Riva, P. Gasco, C. Musicanti, J. Casas, G. Fabrias, R. Ghidoni, P. Signorelli, Anti-inflammatory action of lipid nanocarrier-delivered myriocin: therapeutic potential in cystic fibrosis, Biochim. Biophys. Acta 2014 (1840) 586–594.
[20] A. Mingione, E. Ottaviano, M. Barcella, I. Merelli, L. Rosso, T. Armeni, N. Cirilli, R. Ghidoni, E. Borghi, P. Signorelli, Cystic fibrosis defective response to infection involves autophagy and lipid metabolism, Cells 9 (2020).
[21] A.S. Rambold, S. Cohen, J. Lippincott-Schwartz, Fatty acid trafficking in starved cells: regulation by lipid droplet lipolysis, autophagy, and mitochondrial fusion dynamics, Dev. Cell 32 (2015) 678–692.
[22] E. Jarc, T. Petan, A twist of FATe: lipid droplets and inflammatory lipid mediators, Biochimie 169 (2020) 69–87.
[23] R. Singh, S. Kaushik, Y. Wang, Y. Xiang, I. Novak, M. Komatsu, K. Tanaka, A. M. Cuervo, M.J. Czaja, Autophagy regulates lipid metabolism, Nature 458 (2009) 1131–1135.
[24] S. Kaushik, A.M. Cuervo, Degradation of lipid droplet-associated proteins by chaperone-mediated autophagy facilitates lipolysis, Nat. Cell Biol. 17 (2015) 759–770.
[25] T.B. Nguyen, S.M. Louie, J.R. Daniele, Q. Tran, A. Dillin, R. Zoncu, D.K. Nomura, J. A. Olzmann, DGAT1-dependent lipid droplet biogenesis protects mitochondrial function during starvation-induced autophagy, Dev. Cell 42 (2017) 9–21 (e25).
[26] K. Ouchi, S. Yoshie, M. Miyake, A. Hazama, Cl- channels regulate lipid droplet formation via Rab8a expression during adipocyte differentiation, Biosci. Biotechnol. Biochem. 84 (2020) 247–255.
[27] A. Mingione, C. Verdelli, S. Ferrero, V. Vaira, V. Guarnieri, A. Scillitani, L. Vicentini, G. Balza, E. Beretta, A. Terranegra, G. Vezzoli, L. Soldati, S. Corbetta, Filamin a is reduced and contributes to the CASR sensitivity in human parathyroid tumors, J. Mol. Endocrinol. 58 (2017) 91–103.
[28] A. Dobin, C.A. Davis, F. Schlesinger, J. Drenkow, C. Zaleski, S. Jha, P. Batut, M. Chaisson, T.R. Gingeras, STAR: ultrafast universal RNA-seq aligner, Bioinformatics 29 (2013) 15–21.
[29] Y. Liao, G.K. Smyth, Shi W: featureCounts: an efficient general purpose program for assigning sequence reads to genomic features, Bioinformatics 30 (2014) 923–930.
[30] M.D. Robinson, D.J. McCarthy, Smyth GK: edgeR: a Bioconductor package for differential expression analysis of digital gene expression data, Bioinformatics 26 (2010) 139–140.
[31] G. Yu, L.G. Wang, Y. Han, He QY: clusterProfiler: an R package for comparing biological themes among gene clusters, Omics : a journal of integrative biology 16 (2012) 284–287.
[32] A. Arocho, B. Chen, M. Ladanyi, Q. Pan, Validation of the 2-DeltaDeltaCt calculation as an alternate method of data analysis for quantitative PCR of BCR-ABL P210 transcripts, Diagnostic molecular pathology : the American journal of surgical pathology, part B 15 (2006) 56–61.
[33] D. Bryant, Y. Liu, S. Datta, H. Hariri, M. Seda, G. Anderson, E. Peskett, C. Demetriou, S. Sousa, D. Jenkins, P. Clayton, M. Bitner-Glindzicz, G.E. Moore, W. M. Henne, P. Stanier, SNX14 mutations affect endoplasmic reticulum-associated neutral lipid metabolism in autosomal recessive spinocerebellar ataxia 20, Hum. Mol. Genet. 27 (2018) 1927–1940.
[34] M.P. Ordonez, E.A. Roberts, C.U. Kidwell, S.H. Yuan, W.C. Plaisted, L.S. Goldstein, Disruption and therapeutic rescue of autophagy in a human neuronal model of Niemann pick type C1, Hum. Mol. Genet. 21 (2012) 2651–2662.
[35] J.G. Granneman, H.P. Moore, E.P. Mottillo, Z. Zhu, L. Zhou, Interactions of perilipin-5 (Plin5) with adipose triglyceride lipase, J. Biol. Chem. 286 (2011) 5126–5135.
[36] H. Wang, M. Becuwe, B.E. Housden, C. Chitraju, A.J. Porras, M.M. Graham, X. N. Liu, A.R. Thiam, D.B. Savage, A.K. Agarwal, A. Garg, M.J. Olarte, Q. Lin, F. Frohlich, H.K. Hannibal-Bach, S. Upadhyayula, N. Perrimon, T. Kirchhausen, C. S. Ejsing, T.C. Walther, R.V. Farese, Seipin is required for converting nascent to mature lipid droplets, eLife 5 (2016).
[37] K.M. Szymanski, D. Binns, R. Bartz, N.V. Grishin, W.P. Li, A.K. Agarwal, A. Garg, R. G. Anderson, J.M. Goodman, The lipodystrophy protein seipin is found at endoplasmic reticulum lipid droplet junctions and is important for droplet morphology, Proc. Natl. Acad. Sci. U. S. A. 104 (2007) 20890–20895.
[38] S.A. Onate, S.Y. Tsai, M.J. Tsai, B.W. O'Malley, Sequence and characterization of a coactivator for the steroid hormone receptor superfamily, Science 270 (1995) 1354–1357.
[39] H. Chen, R.J. Lin, R.L. Schiltz, D. Chakravarti, A. Nash, L. Nagy, M.L. Privalsky, Y. Nakatani, R.M. Evans, Nuclear receptor coactivator ACTR is a novel histone acetyltransferase and forms a multimeric activation complex with P/CAF and CBP/p300, Cell 90 (1997) 569–580.
[40] C. Qi, Y. Zhu, J.K. Reddy, Peroxisome proliferator-activated receptors, coactivators, and downstream targets, Cell Biochem. Biophys. 32 (Spring) (2000) 187–204.
[41] C.K. Glass, M.G. Rosenfeld, The coregulator exchange in transcriptional functions of nuclear receptors, Genes Dev. 14 (2000) 121–141.
[42] Y. Jia, C. Qi, P. Kashireddi, S. Surapureddi, Y.J. Zhu, M.S. Rao, D. Le Roith, P. Chambon, F.J. Gonzalez, J.K. Reddy, Transcription coactivator PBP, the peroxisome proliferator-activated receptor (PPAR)-binding protein, is required for PPARalpha-regulated gene expression in liver, J. Biol. Chem. 279 (2004) 24427–24434.
[43] C. Adams, V. Icheva, C. Deppisch, J. Lauer, G. Herrmann, U. Graepler-Mainka, S. Heyder, E. Gulbins, J. Riethmueller, Long-term Pulmonal therapy of cystic fibrosis-patients with amitriptyline, Cellular Physiol. and Biochem. 39 (2016) 565–572.
[44] H.J. Kwon, L. Abi-Mosleh, M.L. Wang, J. Deisenhofer, J.L. Goldstein, M.S. Brown, R.E. Infante, Structure of N-terminal domain of NPC1 reveals distinct subdomains for binding and transfer of cholesterol, Cell 137 (2009) 1213–1224.
[45] V. Choudhary, N. Ojha, A. Golden, W.A. Prinz, A conserved family of proteins facilitates nascent lipid droplet budding from the ER, J. Cell Biol. 211 (2015) 261–271.
[46] B. Kadereit, P. Kumar, W.J. Wang, D. Miranda, E.L. Snapp, N. Severina, I. Torregroza, T. Evans, D.L. Silver, Evolutionarily conserved gene family important for fat storage, Proc. Natl. Acad. Sci. U. S. A. 105 (2008) 94–99.
[47] S. Datta, Y. Liu, H. Hariri, J. Bowerman, W.M. Henne, Cerebellar ataxia disease-associated Snx14 promotes lipid droplet growth at ER-droplet contacts, J. Cell Biol. 218 (2019) 1335–1351.
[48] N. Akizu, V. Cantagrel, M.S. Zaki, L. Al-Gazali, X. Wang, R.O. Rosti, E. Dikoglu, A. B. Gelot, B. Rosti, K.K. Vaux, E.M. Scott, J.L. Silhavy, J. Schroth, B. Copeland, A. E. Schaffer, P.L. Gordts, J.D. Esko, M.D. Buschman, S.J. Field, G. Napolitano, G. M. Abdel-Salam, R.K. Ozgul, M.S. Sagiroglu, M. Azam, S. Ismail, M. Aglan, L. Selim, I.G. Mahmoud, S. Abdel-Hadi, A.E. Badawy, A.A. Sadek, F. Mojahedi, H. Kayserili, A. Masri, L. Bastaki, S. Temtamy, U. Muller, I. Desguerre, J.L. Casanova, A. Dursun, M. Gunel, S.B. Gabriel, P. de Lonlay, J.G. Gleeson, Biallelic mutations in SNX14 cause a syndromic form of cerebellar atrophy and lysosome-autophagosome dysfunction, Nat. Genet. 47 (2015) 528–534.
[49] S. Mandard, M. Muller, S. Kersten, Peroxisome proliferator-activated receptor alpha target genes, CMLS 61 (2004) 393–416.
[50] L. Poulsen, M. Siersbaek, S. Mandrup, PPARs: fatty acid sensors controlling metabolism, Semin. Cell Dev. Biol. 23 (2012) 631–639.
[51] N.E. Wolins, B.K. Quaynor, J.R. Skinner, A. Tzekov, M.A. Croce, M.C. Gropler, V. Varma, A. Yao-Borengasser, N. Rasouli, P.A. Kern, B.N. Finck, P.E. Bickel, OXPAT/PAT-1 is a PPAR-induced lipid droplet protein that promotes fatty acid utilization, Diabetes 55 (2006) 3418–3428.
[52] E. Jarc, T. Petan, Lipid droplets and the Management of Cellular Stress, The Yale journal of biology and medicine 92 (2019) 435–452.